# Global proteome response of *Synechocystis* 6803 to extreme copper environments applied to control the activity of the inducible *petJ* promoter

*Martina Angeleri*[a], *Dorota Muth-Pawlak*[a], *Annegret Wilde*[b], *Eva-Mari Aro*[a] *and Natalia Battchikova*[a]#

[a]*Molecular Plant Biology, Department of Biochemistry, University of Turku, Turku, Finland*

[b]*Molecular Genetics of Prokaryotes, University of Freiburg, D-79104 Freiburg, Germany*

**RUNNING HEAD:** $Cu^{2+}$ treatment for $P_{petJ}$ regulation

# Molecular Plant Biology, Department of Biochemistry, University of Turku, FI-20014 Turku, Finland. Address correspondence to: natbat@utu.fi

13 **ABSTRACT**

14 **Aims**: Cyanobacteria are prokaryotes performing oxygenic photosynthesis, and they can be engineered to harness 15 solar energy for production of commodity and high-value chemicals by means of synthetic biology. The $Cu^{2+}$-16 regulated *petJ* promoter ($P_{petJ}$), which controls the expression of the endogenous cytochrome c553, can be used for 17 expression of foreign products in *Synechocystis* 6803. We aimed to disclose potential bottlenecks in application of 18 the $P_{petJ}$ in synthetic biology approaches. **Methods and Results**: Quantitative label-free mass spectrometry 19 revealed global proteome changes which occurred during nutrient conditions which repress or activate of $P_{petJ}$ in 20 *Synechocystis* 6803. **Conclusions:** Some irreversible proteome alterations were discovered due to the copper 21 stress, including down-regulation of the ribosomal proteins, significant changes in proteins amounts of the cell 22 surface layer and the outer and inner membranes. **Significance and Impact of Study**: This study revealed 23 limitations in the use of $P_{petJ}$ for biotechnological applications.

24

25 **KEYWORDS**: cyanobacteria, *Synechocystis*, biotechnology, bioproduct, *petJ* promoter, copper stress response, 26 proteomics, quantitative label-free mass spectrometry.

27

28 **INTRODUCTION**

29 Presently, many efforts are directed to development of sustainable production platforms and circular
30 economy. Some living organisms, like green plants and algae, convert sunlight into chemical energy and reducing
31 equivalents to support growth and concomitantly release oxygen in the process known as oxygenic photosynthesis.
32 Using synthetic biology approaches, they can be engineered to harness solar energy for production of commodity
33 and high-value chemicals. Cyanobacteria are the only prokaryotes which perform oxygenic photosynthesis, and
34 many of them can be easily genetically manipulated. Therefore, they are prospective organisms to be used as
35 chassis for heterologous expression of proteins and metabolic pathways of interest (Phillips and Silver 2006;
36 Parmar *et al.* 2011; Aro 2016). Proof of concept for light-driven production of exogenous proteins and chemicals
37 has already been demonstrated in engineered cyanobacterial strains (Gudmundsson and Nogales 2015). However,
38 synthesis of foreign compounds has been shown to compete with natural carbon partitioning in growing cells
39 (Schuurmans *et al.* 2017; Giordano and Wang 2018). The carbon partitioning and product yields differ in various
40 growth phases (Wang *et al.* 2016; Schuurmans *et al.* 2017). For instance, enhanced production is obtained by
41 metabolically active cells in the absence of growth (Berla *et al.* 2013). Thus, a favourable partition of the carbon
42 flux into a desirable product can be achieved by in-time separation of biomass accumulation from the production
43 of a target compound (Phillips and Silver 2006; Murthy *et al.* 2014). One of the key elements of this
44 approach is the use of inducible promoters for gene expression. Therefore, the selection of an optimal promoter is
45 an important step in designing the scheme for genetic manipulation of chassis cells by insertion of heterologous
46 genes and metabolic pathways.

47 *Synechocystis* sp. PCC 6803 (hereafter *Synechocystis*) is widely used as a model organism for
48 investigations directed to production of chemicals and biofuels by synthetic biology approaches (Phillips and
49 Silver 2006; Hagemann and Hess 2018). Only few inducible promoters are available and utilized for production
50 of valuable chemicals in this strain as well as in other cyanobacteria (Heidorn *et al.* 2010; Berla *et al.* 2013;
51 Englund *et al.* 2016; Ferreira *et al.* 2018). One of them is the *petJ* promoter ($P_{petJ}$) which can be regulated by
52 varying concentrations of $Cu^{2+}$ ions present in the growth medium (Diaz *et al.* 1994; Mitschke *et al.* 2011; Eisenhut
53 *et al.* 2012; Kuchmina *et al.* 2012; Gandini *et al.* 2017; Pade *et al.* 2017). The *petJ* gene encodes the endogenous

54 cytochrome $c_{553}$ (cyt $c_{553}$), a protein which functions as the soluble photosynthetic electron carrier in $Cu^{2+}$ limiting
55 conditions (Sandmann 1986; Zhang *et al.* 1992; Diaz *et al.* 1994). When $Cu^{2+}$ is available, *petJ* is not expressed,
56 and the cyt $c_{553}$ protein is substituted by plastocyanin (PC) which is encoded by the *petE* gene. The *petJ* promoter
57 is partially active in standard BG-11 medium (0.3 µmol $l^{-1}$ $Cu^{2+}$) (Stanier *et al.* 1971; Rippka *et al.* 1979). However,
58 it can be completely repressed by an excess of $Cu^{2+}$ ions (5 µmol $l^{-1}$ ) in the growth medium, or fully induced by
59 elimination of $Cu^{2+}$ (0 µmol $l^{-1}$) from the extracellular environment. The $P_{petE}$ promoter is regulated in the opposite
60 way (Zhang *et al.* 1992; Diaz *et al.* 1994). Therefore, both $P_{petJ}$ and $P_{petE}$ are considered to be suitable for
61 overexpression of various genes in biotechnological applications (Kuchmina *et al.* 2012; Klähn *et al.* 2015).

62 Nevertheless, it is important to keep in mind that the cyanobacterial chassis cells are living organisms with
63 a complex metabolic network. Therefore, introduction of a foreign genetic element by synthetic biology
64 approaches and/or changing the growth conditions utilized for controlling the promoter activity most probably
65 would cause rearrangements of intracellular metabolic pathways (Gudmundsson *et al.* 2018). This, in turn, might
66 affect the expression of the introduced genetic element and/or accumulation of the product of interest (Giordano
67 and Wang 2018). Here we investigated how the *Synechocystis* proteome responded to conditions which repress
68 $P_{petJ}$ followed by activation of the promoter. This was reached by supplying excess of copper ions to the growth
69 medium, followed by shifting the cells a copper-free environment. To this end, we carried out label-free liquid
70 chromatography-tandem mass spectrometry (LC-MS/MS) quantitative analysis of a *Synechocystis* strain carrying
71 an empty self-replicating vector with the *petJ* promoter. The experiment imitated in-time separation of the growth
72 and biomass accumulation phase from the target protein production phase, with repressed and activated $P_{petJ}$,
73 respectively. Cells were not producing a foreign compound. The obtained results provide insights into metabolic
74 pathways that are affected even in the absence of introduced foreign genes and, therefore, might become a
75 bottleneck in real biotechnological experiments.

## MATERIAL AND METHODS

### Growth conditions

*Synechocystis* 6803 PCC-M (Trautmann *et al.* 2012) harbouring the conjugative plasmid pVZ321 (Zinchenko *et al.* 1999) with kanamycin (Km)- and chloramphenicol (Cm)-resistance cassettes (Mitschke *et al.* 2011) was used in the present study. Cells were grown at 30°C, under constant illumination of 50 µmol photons$^{-2}$ s$^{-1}$, in atmospheric air, in media supplemented with 40 µg ml$^{-1}$ Km, 7 µg ml$^{-1}$ Cm. The content of the growth medium differed at distinct stages of the experiment. Control cells were incubated in the ordinary BG-11 medium (standard condition, 0.3 µmol l$^{-1}$ $Cu^{2+}$; Rippka *et al.* 1994). The aliquots of cells grown in standard condition (S) to $OD_{750}$ ~1 were taken for the proteome analysis. At the 1st step of the experiment, cells were shifted to high $Cu^{2+}$ concentration (5 µmol l$^{-1}$) as follows. Cells grown in standard condition were diluted to OD750 ~0.2 with BG-l1 medium containing 1 µmol l$^{-1}$ $Cu^{2+}$. After 1-day incubation, $CuSO_4$ was added to 2.5 µmol l$^{-1}$, and after 2 days, $Cu^{2+}$ concentration was finally increased to 5 µmol l$^{-1}$. When high $Cu^{2+}$-grown cells reached OD750 ~1, the aliquots (H) were collected for the proteome analysis. At the 2nd step of the experiment, the high $Cu^{2+}$ -grown cells were washed with $Cu^{2+}$-free BG-11 medium, grown in this medium for two days to OD750 ~1, and collected for protein analysis as $Cu^{2+}$ depleted cells (D). The experiment was performed with three biological replicates.

### Protein isolation and digestion to peptides

*Synechocystis* cells were collected by centrifugation at 4000 ***g*** at 4°C for 10 minutes and washed twice with 50 mmol l$^{-1}$ triethylammonium bicarbonate buffer (TEAB; Sigma-Aldrich, Missouri, United States) (pH 8.0). Cell pellets were re-suspended in a buffer containing 8 mol l$^{-1}$ urea, 100 mmol l$^{-1}$ TEAB pH 8.0, 4 mmol l$^{-1}$ 1,4-Dithiothreitol (DTT; Sigma-Aldrich, Missouri, United States) and 0.2 mmol l$^{-1}$ phenylmethylsulfonyl fluoride (PMSF; Roche, Basel, Switzerland) and broken with an equal volume of glass beads in the mixer mill MM400 (Retsch Inc, Haan, Germany), using three subsequent cycle at 30 Hz, 4°C for 10 min. To facilitate extraction of membrane proteins, sodium dodecyl sulphate (SDS; Avantor-VWR, Pennsylvania, United States) was added to the lysates to a final concentration of 0.1% and incubated at RT for 30 min. Cell debris was removed by centrifugation at 11000 ***g***, RT for 30 min. Protein concentration was determined using Pierce™ BCA Protein Assay (Thermo Fisher Scientific, Massachusetts, United States). For proteomic analyses, 100 µg of proteins were purified

102 and treated as follows. The proteins were precipitated with 6 volumes of acetone at −20 °C overnight and
103 centrifuged at 11000 ***g***, 4°C for 30 min. The pellets were dissolved in the buffer containing 6 mol $l^{-1}$ urea, 25 mmol
104 $l^{-1}$ ammonium bicarbonate buffer (ABC) pH 7.5, 0.1% RapiGest FS (Waters Corporation, Massachusetts, United
105 States). Proteins were reduced with 10 mmol $l^{-1}$ DTT at 30 C for 1 h and alkylated with 35 mmol $l^{-1}$ iodoacetamide
106 (IAA) (Sigma-Aldrich, Missouri, United States) at RT for 1h followed by dilution with 4 volumes of the same
107 buffer without urea. The digestion of protein with Trypsin Gold (Promega, Wisconsin, United States) was
108 performed at 30°C overnight. The tryptic digests were acidified to pH ≈ 2 using formic acid (FA) (Sigma-Aldrich,
109 Missouri, United States) and incubated at 37 °C for 30 min. RapiGest FS degradation products were removed by
110 centrifugation at 11000 ***g***, RT, for 30 min. The peptides were desalted using C18 cartridges (Sep-Pack, 50 mg, 3cc,
111 Waters Corporation, Massachusetts, United States) according to the manufacturer's protocol. The eluted peptides
112 were lyophilized in SpeedVac (Savant SPD1010, Thermo Fisher Scientific, Massachusetts, United States),
113 solubilized in 1% FA, 2% acetonitrile (AcN) and stored at -80 °C prior to LC-MS/MS analyses.

114 **LC−MS/MS Analysis**

115 Equivalents of 200 ng of peptides were injected in the LTQ Orbitrap Velos Pro mass spectrometer (Thermo Fisher
116 Scientific, Massachusetts, United States) with the electrospray ionization source connected in-line with a nano-
117 HPLC (high-performance liquid chromatography) system (EasyNanoLC 1000, Thermo Fisher Scientific,
118 Massachusetts, United States). Peptides were separated on a C18 pre-column (5 x 0.3 mm, PepMap C18, LC
119 Packings) and a C18 nano-column (15 cm x 75 µm, Magic 5 µm 200 Å C18, Michrom BioResources Inc.,
120 Sacramento, CA, USA) with a flow rate of 300 nL $min^{-1}$ using 0.2% FA, 2% AcN as a buffer A and 0.2% FA,
121 95% AcN as a buffer B. To separate the peptide mixture, 110-min gradient was applied as follows: from 2% to
122 20% B in 70 min, from 20% to 40% B in 30 min, 100% B for 10 min. MS data were acquired automatically in the
123 positive mode with 2.3 kV ionization potential using the Thermo Xcalibur software (Thermo Fisher Scientific,
124 Massachusetts, United States). The data-dependent acquisition (DDA) mass spectrometry method combined MS
125 survey scans of mass range 300-2000 m $z^{-1}$ and MS/MS scans for up to ten most intensive +2 or +3 charged peptide
126 ions; fragmentation was performed by collision-induced dissociation (CID), with normalized collision energy of

127 35 %. The spectra were registered with resolution of 60000 and 17500 (at m $z^{-1}$ 200) for full scan and for fragment
128 ions, respectively.

129 **Protein identification and quantitation**

130 The raw files were analysed using the Mascot (v. 2.4) search engine (Perkins et al 1999) and Proteome
131 Discoverer™ (v.1.4) Software (Thermo Fisher Scientific, Massachusetts, United States). The *Synechocystis* 6803
132 protein database used in the searches was retrieved from Cyanobase (Kaneko *et al.* 1996;
133 http://genome.microbedb.jp/cyanobase) and supplemented with the list of common laboratory contaminants.
134 Following search criteria were applied: trypsin as enzyme, two miscleavages allowed, carbamidomethylation as
135 the fixed modification and methionine oxidation as variable one. Precursor mass tolerance was restricted to ±10
136 ppm for precursor ions and to ±0.8 Da for fragment ions. For the validation of spectra identifications, Percolator
137 algorithm was used with relaxed false discovery rate (FDR) of 0.05. Three biological replicates were assessed for
138 each growth condition, and protein abundances were estimated based on area of the peaks representing
139 corresponding peptides (Grouneva *et al.* 2016; Huokko *et al.* 2017). Proteins were identified with at least two
140 unique peptides; few proteins identified based on one peptide were included, too, after manual examination. Global
141 label-free protein quantitation was performed using Progenesis QI for proteomics software v. 4.0 (Nonlinear
142 Dynamics, Newcastle upon Tyne, UK). All non-conflicting peptides identified with ±10 ppm mass error for a
143 precursor were taken into account. At the protein level, the statistical significance threshold in Anova was set to
144 $p<0.05$. The practical significance threshold for differential expression was set to FC of +/- 1.4. Protein annotation
145 is given according to Cyanobase; in some cases, manual curation of annotation was performed based on available
146 literature. When functional information was discovered for proteins annotated in Cyanobase as “hypothetical” or
147 “unknown”, the proteins were moved to a corresponding category.

148 **RESULTS**

149 **Experimental setup**

150 The scheme of the experiment mimicking the expression of heterologous protein(s) under control of the
151 *petJ* promoter, here conducted with an empty vector, is shown in Fig 1. The control cells were grown in the

152 ordinary BG-11 medium (Rippka *et al.* 1979) (S in Fig 1). The 1st step of the experiment reflected the repression

153 of the *petJ* promoter by high $Cu^{2+}$ concentration. Here, cells grown under standard conditions (0.3 µmol $l^{-1}$ $Cu^{2+}$)

154 were gradually adjusted to high $Cu^{2+}$ concentration (5 µmol $l^{-1}$) (H in Fig 1) where the *petJ* promoter is fully

155 repressed (Georg *et al.* 2014). It is important to note that he gradual addition of copper ions (described in detail in

156 Materials and Methods) was applied to let cells to acclimate to the toxic $Cu^{2+}$ concentration (>3 µmol $l^{-1}$; Zhang

157 *et al.* 1992; Giner-Lamia *et al.* 2014) and thus to avoid the known harmful effect of an abrupt shift of cyanobacteria

158 to medium with high amounts of $Cu^{2+}$. The 2nd step of the experiment reflected the induction of the *petJ* promoter

159 by $Cu^{2+}$ depletion; here, cells incubated at high $Cu^{2+}$ concentration were shifted to copper-free BG-11 medium (D

160 in Fig 1) and incubated for 2 days to achieve maximal $P_{petJ}$-dependent expression (Eisenhut *et al.* 2012). The

161 activation of the *petJ* promoter would lead to the production of a potential product in a real biotechnological

162 experiment. However, no foreign protein(s) were produced in these cells, and all proteome changes during the

163 course of the experiment should be attributed to the conditions administered to simulate a production process using

164 the *petJ* promoter. The changes in OD values during the experiment are shown in Fig.S1. Please note that cells in

165 all three conditions, S, H, and D, were collected for proteomic analysis at the same OD value of about 1, to avoid

166 influence of other environmental effects, for example self-shading.

167 **Relative protein quantitation**

168 Protein preparations from cells collected in S, H, and D growth phases (Fig 1) were analysed in parallel

169 using the label-free LC-MS/MS proteomic approach (Bantscheff *et al.* 2007; Grouneva *et al.* 2016; Huokko *et al.*

170 2017). Relative H/S quantitation demonstrated proteome modifications which occurred at the stage of biomass

171 accumulation and were caused by increased $Cu^{2+}$ concentration. Relative D/H changes reflected the response of

172 *Synechocystis* proteome to the removal of $Cu^{2+}$ from the growth medium causing activation of $P_{petJ}$. Finally, relative

173 D/S quantitation revealed ultimate changes in the *Synechocystis* proteome which would occur in real

174 biotechnological experiments independently on the production of the heterologous protein(s) under control of the

175 *petJ* promoter.

176 In the experiment, 1736 proteins were identified, and 812 of them were quantified with the P-value of

177 0.05. For each quantified protein, the number of peptides, the average fold change (FC) values in three replicas

178 and Anova, are presented in the Table S1. The numbers of proteins with significantly altered expression (FC of ± 179 1.40) at distinct stages of the experiment are showed in Table 1. The corresponding proteins are listed in the Table 180 2 and Table S2.

181 **$Cu^{2+}$ homeostasis**

182 As expected, proteins responsible for the $Cu^{2+}$ homeostasis were strongly affected by changes in the 183 concentration of the metal ion. Upon addition of 5 μmol $l^{-1}$ $CuSO_4$, the proteins encoded by the *copMRS* operon 184 showed strong up-regulation, up to 40-fold increase for the CopR protein which, together with CopS, constitute 185 the two-component Hik31/Rre34 system mediating a tightly controlled $Cu^{2+}$ resistance mechanism. Noteworthy, 186 *Synechocystis* encodes two *copMRS* operons, one on the chromosome (*sll0788-sll0790*) and another on the 187 endogenous pSYSX plasmid (*slr6039-slr6041*). The corresponding proteins in these operons are highly similar 188 (95% identity, Giner-Lamia *et al.* 2012); therefore, collected MS/MS data did not allow to differentiate between 189 them. The *copBAC* operon (*slr6042-slr6044*) encoding the transport system, which exports the surplus of $Cu^{2+}$ 190 from periplasm and the cytosol (Giner-Lamia *et al.* 2012), and the small soluble copper metallochaperone Atx1 191 (Ssr2857) which helps to avoid misallocation of the reactive $Cu^{1+}$ and aberrant interaction with other enzymes, 192 such as zinc or cobalt transporters (Tottey *et al.* 2008; Tottey *et al.* 2012), were also up-regulated at high $Cu^{2+}$ 193 concentration.

194 When $Cu^{2+}$ was removed from the growth medium, the proteins of the copper homeostasis described above 195 showed the opposite effect, being down-regulated in the depleted conditions compared to high $Cu^{2+}$ concentration. 196 Despite the obvious decrease in accumulation after 2 days of growth in the $Cu^{2+}$-free medium, the proteins 197 remained slightly up-regulated compared to the levels in the beginning of the experiment, except CopA which 198 dropped below levels observed in standard BG-11.

199 **Photosynthesis-related proteins**

200 The alterations in the intracellular concentration of $Cu^{2+}$ were reflected also in differential expression of 201 the two photosynthetic proteins PC (Sll0199) and cyt $c_{553}$ (Sll1796) at the different stages of the experiment. The 202 expression of the two soluble electron carriers which is known to be directly regulated by $Cu^{2+}$ availability (Zhang 203 *et al.* 1992; Giner-Lamia *et al.* 2014; Giner-Lamia *et al.* 2016) demonstrated reverse behaviour. During $Cu^{2+}$

204 excess, PC was strongly up-regulated, and cyt $c_{553}$ was markedly down-regulated. Upon $Cu^{2+}$ depletion, their
205 dynamics was reversed, and the drastic up-regulation of cyt $c_{553}$ indicated that two days of growth in $Cu^{2+}$-depleted
206 medium were sufficient to efficiently activate the *petJ* promoter.

207 The thylakoid-embedded complexes involved in linear electron flow were distinctly affected by the shift
208 in the $Cu^{2+}$ concentration. For PsaE (Ssr2831) and PsaL (Slr1655) of photosystem I (PSI), down-regulation was
209 observed at 5 µmol $l^{-1}$ $Cu^{2+}$, and their accumulation did not recover under copper-limiting conditions. The same
210 effect was observed for PetB (Slr0342) representing the cytochrome $b_6f$ (cyt $b_6f$) complex. Similar tendency was
211 noticed for some other subunits of PSI, photosystem II (PSII), cyt $b_6f$, and the phycobilisome (PBS) antenna (Table
212 S1). The cooperative down-regulation of several proteins directly involved in light harvesting and linear electron
213 flow, which was detected at the end of the experiment compared to the standard level, might indicate that some
214 irreversible damage occurred to the photosynthesis machinery during treatment of cells with 5 µmol $l^{-1}$ $Cu^{2+}$.
215 Ferredoxin I (Ssl0020) which functions as the acceptor of photosynthesis-derived electrons, was up-regulated at
216 high $Cu^{2+}$ but its accumulation diminished at the depletion stage.

217 The synthesis of chlorophyll and porphyrins, the pigments which are vital for the photosynthetic activity,
218 was also affected, especially during acclimation to high $Cu^{2+}$. HemF (Sll1185), HemB (Sll1994) and HemL
219 (Sll0017) participating in conversion of glutamate to protoporphyrin IX, ChlP (Sll1091) which catalyses the last
220 step of bacteriochlorophyll synthesis, and heme oxidase Hox1 (Sll1184) were down-regulated, in line with
221 reduction of the photosynthetic protein complexes. HemL remained at low levels also upon $Cu^{2+}$ removal.

222 Various dynamics were observed for proteins involved in photoprotection, regulation of photosynthesis
223 and biogenesis of photosystems. Up-regulation during the high $Cu^{2+}$ phase was detected for proteins of the PSII
224 assembly proteins (PAP) operon (Slr0144, Slr0147, Slr0149, Slr0151) known to be induced by high light and
225 involved in PSII (Wegener *et al.* 2008; Yang *et al.* 2014; Rast *et al.* 2016) and PSI (Kubota *et al.* 2010)
226 biosynthesis, Slr1768 with a structural role in maintaining thylakoid membranes under high light (Bryan *et al.*
227 2011), and membrane-associated rubredoxin A (Slr2033) essential for PSII assembly (Calderon *et al.* 2013). In
228 contrast, accumulation of flavodiiron proteins Flv2 and Flv4 (Slr0219 and Slr0217), which safeguard PSII in

229 *Synechocystis* cells (Bersanini *et al.* 2014), dropped at high $Cu^{2+}$ but returned to the standard levels upon removing

230 the metal ions from the growth medium.

231 **Carbon and nitrogen metabolism and transporters**

232 In line with suppression of photosynthetic proteins, high $Cu^{2+}$ conditions disturbed the carbon uptake

233 causing down-regulation of the high affinity $HCO_3^-$ transporter (BCT-1) encoded by the *cmpABCD* operon. All

234 three quantified subunits (CmpB, Slr0041; CmpC, Slr0043; CmpD, Slr0044) of the transporter were reduced by

235 50% at 5 µmol $l^{-1}$ $Cu^{2+}$. The structure of carboxysomes, where $CO_2$ fixation takes place, was possibly affected

236 since the CcmK2 shell protein (Sll1028) was up-regulated while its analogue, CcmK4 (Slr1839), was reduced. At

237 the depletion stage, the amounts of the BCT-1 transporter returned back to the standard levels, but the CcmK2 up-

238 regulation increased, and the CcmM protein (Sll1031), involved in early steps of the carboxysome biogenesis, was

239 reduced at the end of the experiment. Various dynamics were observed for some emzymes of the TCA cycle (CitH,

240 Sll0891; SucD, Sll1557), glycolysis/glyconeogenesis (Fbp, Slr0952; Pgm, Sll0395), the pentose phosphate cycle

241 (CfxE, Sll0807), formation of the polyhydroxybutyrate granules (the phasine protein, Ssl2501); however, a

242 majority of proteins which belong to the central carbon metabolism were not strongly affected by changes of the

243 $Cu^{2+}$ concentration (Table S1).

244 In contrast, nitrogen uptake and assimilation were strongly intensified at high $Cu^{2+}$ concentration.

245 Glutamine synthetase (GS) type III (Slr0288), otherwise named as glutamate-ammonia ligase GlnN and shown to

246 be highly up-regulated in condition of nitrogen starvation (Reyes *et al.* 1997), was one of the most strongly induced

247 enzymes. In line, the GS-inactivating factors IF7 (Ssl1911) and IF17 (Sll1515) were down-regulated in high $Cu^{2+}$,

248 with the former being the most negatively affected protein detected in this study. Further, components of the

249 nitrite/nitrate transport system were up-regulated in 5 µmol $l^{-1}$ $Cu^{2+}$, including NtrB (Sll1451), NtrC (Sll1452) and

250 NtrD (Sll1453) as well as ferredoxin-nitrite reductase NirA (Slr0898). An additional nitrogen uptake was provided

251 by up-regulation of urea transporter proteins UrtA (Slr0447), UrtC (Sll1201) and UrtD (Sll0764), the urease

252 subunits *beta* and *gamma* (Slr1256 and Sll0420, respectively) and the cyanate lyase (Slr0899). On the other hand,

253 the urease-related UreG protein (Sll0643) was down-regulated. Upon $Cu^{2+}$ depletion, majority of proteins involved

254 in nitrite/nitrate and urea transport return to the standard levels. However, GS GlnN remained up-regulated and
255 both GS-inactivation factors IF7 and IF17 stayed down-regulated.

256 **Protein synthesis and degradation**

257 Importantly, ribosomal proteins were affected during the experiment. Some of them were repressed at the
258 stage of acclimation to high $Cu^{2+}$, some were decreased upon $Cu^{2+}$ depletion, but in the end several ribosomal
259 proteins demonstrated marked down-regulation. Similar tendency was observed for translation initiation factors
260 IF-1 (Ssl3441), IF-2 (Slr0744) and IF-3 (Slr0974). Further, the elongation factor P (Slr0434) involved in translation
261 was also down-regulated in high $Cu^{2+}$ media. Upon switch of cells from high $Cu^{2+}$ to $Cu^{2+}$-depleted growth
262 medium, amounts of proteins involved in the tRNAs synthesis were restored to the standard expression levels but
263 the elongation factor P remained significantly downregulated. In parallel to components of protein synthesis,
264 aminopeptidase P (Sll0136), which is involved in protein degradation, especially in high light and heat conditions
265 (Pojidaeva *et al.* 2013), was down regulated during the high $Cu^{2+}$ phase and further decreased its amount after
266 switching to $Cu^{2+}$-depleted medium. In contrast, the periplasmic peptidase YmxG (Slr1331) responsible for the
267 maturation of periplasmic proteins (Fulda *et al.* 2000) was up-regulated at the end of the experiment.

268 **Cellular periphery**

269 The changes in $Cu^{2+}$ concentration administered to control a potential P*petJ*-driven production process
270 triggered cell wall remodelling and alteration in outer and plasma membrane content. The Slr1704 protein involved
271 in synthesis of external protective S-layer (Huang *et al.* 2004) was highly up-regulated during acclimation to high
272 $Cu^{2+}$ and its accumulation even enhanced at the stage of the $Cu^{2+}$ depletion. Porins Slr1908 and Slr1841, the PilQ
273 protein (Slr1277), a component of the type IV pilus (Yoshihara *et al.* 2001), as well as SynToc75 (Slr1227), one
274 of the proteins of the secretion channels in the outer envelope (Reumann *et al.* 1999; Fulda *et al.* 2002; Huang *et*
275 *al.* 2004), were up-regulated at 5µmol $l^{-1}Cu^{2+}$ and remained at elevated levels despite $Cu^{2+}$ removal from the growth
276 medium. The CccP (Slr1668) and CccS (Slr1667) proteins involved in construction of cell surface components
277 and in motility processes (Yoshimura *et al.* 2010), increased in high $Cu^{2+}$ but returned to normal levels upon the
278 metal ion depletion. Enzymes engaged in peptidoglycan biosynthesis, MurA (Slr0017), MurG (Slr1656), GlmU
279 (Sll0899), and LpdX (Slr0776), demonstrated various dynamics. MurG remained to be strongly up-regulated at

280 the end of the experiment. Diverse transport systems were also affected including the lipopolysaccharide ABC
281 transporter (RfbB, Sll0575), sodium/sulfate symporter Sac1 (Sll0640), the Nat permease for neutral amino acids
282 (NatE, Slr1881), and some others. Several proteins were found to be down-regulated at the end of the experiment,
283 especially ZiaA (Slr0798), the zinc efflux pump involved in zinc tolerance. The strong ZiaA decrease might be
284 caused by misincorporation of the copper ion instead of zinc at 5 µmol $l^{-1}$ $Cu^{2+}$ since these metals compete in
285 binding to proteins (Badarau *et al.* 2011).

286 **Other proteomic perturbations caused by $Cu^{2+}$ treatment**

287 Many other *Synechocystis* proteins responded to changes in $Cu^{2+}$ concentrations. They belong to various
288 functional categories and are involved in multiple metabolic routes. Among them are signalling and regulatory
289 proteins Hik37 (Sll0094), Hik32 (Sll1473), Rre21 (Slr1982) which belong of the two-component signalling
290 systems, the anti-sigma F factor antagonist Slr1859, heat-shock proteins GroES (Slr2075) and DnaJ2 (Slr0093);
291 redox-regulators like glutaredoxin GrxB (Slr1562), glutathione S-transferase Gst1 (Sll1545) and FTR-ferredoxin-
292 thioredoxin reductase FtrV (Ssr0330); metal-binding proteins bacterioferritin BfrA (Sll1341) and iron-sulfur
293 clusters assembly factor NifU (Ssl2667); elements of the secretion machinery RND multidrug efflux transporter
294 AcrF (Slr2131), preprotein translocase SecY subunit (Sll1814), and hemolysin secretion protein HlyD (Sll1181);
295 proteins involved in synthesis of secondary metabolites like thiamine biosynthesis protein ThiG (Slr0633);
296 pyridoxal phosphate biosynthetic protein PdxJ (Slr1779); the polyphosphate kinase (Sll0290) involved in the
297 synthesis of polyphosphate which serves as the inorganic phosphate storage compound; etc. They demonstrated
298 different dynamics of changes during stages of acclimation to high $Cu^{2+}$ and following copper ion depletion.

299 The largest group of proteins affected by the changes in copper concentrations during the experiment
300 included those with unknown functions (Table S2). Many of these proteins were differentially regulated at 5 µmol
301 $l^{-1}$ $Cu^{2+}$ and did not return to the standard levels after the copper ion depletion. Thus, the *Synechocystis* proteome
302 demonstrated significant alterations caused by changes in the availability of copper ions administered to control
303 the $P_{petJ}$ activity.

304 **DISCUSSION**

305 Cyanobacteria are prospective organisms to be used as chassis for light-driven production of exogenous 306 proteins and chemicals. The use of inducible promoters is a popular approach for expression of genes introduced 307 into host cells by synthetic biology techniques (Khalil and Collins 2010). The activity of the *petJ* promoter is 308 controlled by the availability of copper ions in the growth medium: it is partially transcribed in standard BG-11 309 (0.3 µmol $l^{-1}$ $Cu^{2+}$); it is completely repressed at 5 µmol $l^{-1}$ of $Cu^{2+}$, and it is fully activated in copper-free medium. 310 Therefore, it appears to be a promising choice in biotechnological applications, especially those where the biomass 311 accumulation step is separated from the synthesis of a desirable product, in order to enhance the yield by optimising 312 the carbon partitioning, or due to a negative effect of a product of interest on cell metabolism (Murthy *et al.* 2014).

313 Copper is an essential enzyme cofactor, and cyanobacteria have adapted to its presence in trace amounts 314 in the growth media. However, copper in excess can be toxic for cyanobacteria and cause cell death when high 315 $Cu^{2+}$ concentrations are introduced abruptly (Zhang *et al.* 1992, Giner-Lamia *et al.* 2014). For example, the toxic 316 effect of copper ions has been observed when > 3 µmol $l^{-1}$ $Cu^{2+}$ was added to the copper-free growth medium 317 (Giner-Lamia *et al.* 2012, 2014); thereafter, we denote the sharp and drastic increase of copper concentration in 318 the growth medium as the shock treatment. In contrast, slow acclimation to increasing copper concentrations 319 allows cells to successfully survive in otherwise toxic conditions (Shavyrina *et al.* 2001; Stuart *et al.* 2009; Stuart 320 *et al.* 2017).

321 When the *petJ* promoter is used for biotechnological purposes, the standard procedure includes growing 322 cells at gradually increasing concentration of $Cu^{2+}$ (up to 5 µmol $l^{-1}$ for *Synechocystis*) followed by depletion of 323 the medium from this ion for the efficient synthesis of products of interest. During this procedure, cells undertake 324 profound metabolic rearrangements, first due to the gradual acclimation to the high $Cu^{2+}$ concentration at the 325 biomass accumulation phase, and then due to copper depletion at the production phase. For practical applications, 326 it is important to know whether these rearrangements are reversible, and if not, which functions and metabolic 327 routes are affected. Responses of cyanobacteria to high concentration of metal ions have been extensively 328 investigated due to possibility to use these organisms as environmentally-friendly bioremediation tools (Jamers *et* 329 *al.* 2006), but the relaxation mechanisms are poorly studied (Pereira *et al.* 2011; Kumar 2015).

330 Here we mimicked such a biotechnological experiment with *Synechocystis* cells harbouring an empty
331 expression plasmid. This plasmid was previously used, for instance, to engineer *Synechocystis* to produce ethanol
332 under control of the *petJ* promoter under copper limitation (Dienst *et al.* 2014). Cells grown in standard BG-11
333 medium were first acclimated to the high $Cu^{2+}$ concentration and subsequently exposed to the $Cu^{2+}$-free condition.
334 At all three stages, standard (S, 0.3 µmol $l^{-1}$ $Cu^{2+}$), high $Cu^{2+}$ (H, 5 µmol $l^{-1}$), and depletion (D, 0 µmol $l^{-1}$ $Cu^{2+}$),
335 samples were taken, in triplicates, for global quantitative proteome analysis by the label-free LC-MS/MS
336 technique.

337 **The acclimation of the *Synechocystis* proteome to excess of $Cu^{2+}$**

338 Due to the gradual addition of copper to the growth medium during the S-to-H phase, the cells successfully
339 acclimated to the high concentration of copper ions, 5 µmol $l^{-1}$ $Cu^{2+}$ (Suppl. Fig. 2). The similar increase of copper
340 tolerance during the slow acclimation process has been shown for *Synechococcus* species (Stuart *et al.* 2009; Stuart
341 *et al.* 2017). Thus, by acclimation, we avoided the detrimental, toxic effect of copper ions that has been observed
342 after the shock treatment (Giner-Lamia *et al.* 2012, 2014).

343 Differential expression of proteins at high $Cu^{2+}$ compared to the standard conditions, H/S (Tables 2 and
344 S2), revealed how *Synechocystis* cells acclimated during the gradual increase in copper concentration to the
345 otherwise toxic concentrations of the metal ion. The results are summarized in Fig S2. In line with earlier studies
346 (Zhang *et al.* 1992; Diaz *et al.* 1994; De La Cerda *et al.* 2008; Giner-Lamia *et al.* 2014), cyt $c_{553}$ encoded by the
347 *petJ* gene was strongly down-regulated, indicating that the native *petJ* promoter became indeed repressed. PC,
348 which is the main copper containing protein in *Synechocystis*, was distinctly induced. Significant changes were
349 observed in proteins involved in copper homeostasis. CopR, CopS, and CopM, encoded by the *copMRS* operon,
350 were among the most up-regulated proteins in H. CopR and CopS constitute the two-component Hik31/Rre34
351 system responsible for the copper resistance in *Synechocystis* cells (Giner-Lamia *et al.* 2012). It has been suggested
352 that the CopS protein detects copper directly (Giner-Lamia *et al.* 2012). Thus, CopRS upregulation reflected the
353 increase in the intracellular copper concentration. From other proteins involved in copper homeostasis, CopB and
354 CopC, components of the heavy-metal efflux system, were up-regulated in H, as well as the Atx1 protein, the small
355 chaperonin participating in the intracellular copper transport. From the family of dehydratases that comprise the

356 Fe-S clusters which are considered to be primary targets of the copper toxicity (Macomber *et al.* 2006; Macomber
357 and Imlay 2009; Giner-Lamia *et al.* 2014; Huertas *et al.* 2014), AroQ (Sll1112), 3-dehydroquinate dehydratase
358 involved in biosynthesis of aromatic acids, was strongly up-regulated in high copper-acclimated *Synechocystis*
359 cells.

360 The global response of cyanobacterial cells to high copper concentrations has been investigated in
361 *Synechocystis* (Giner-Lamia *et al.* 2014) and in marine *Synechoccoccus* species (Stuart *et al.* 2009) using
362 transcriptomic approach. In these studies, the cells have been subjected to the $Cu^{2+}$ shock treatment. Results
363 described above, such as the down-regulation of many proteins involved in photosynthesis, chlorophyll
364 biosynthesis, and protein synthesis (Tables 2 and S2), are in line with these investigations. Nevertheless, the
365 changes in the *Synechocystis* proteome pattern in cells acclimated to the high copper condition (Table 2 and Suppl.
366 Table 1) seem to differ from the ones that could be expected from microarray results obtained from the shock-
367 treated cells (Giner-Lamia *et al.* 2014). Most probably, the divergence of the responses is due to the different
368 experimental setup. However, it is also possible that changes in the transcriptome are not reflected in the proteome.
369 Considering the dehydratase family, LeuC (Sll1470) and LeuD (Sll1444), the large and small subunits of 3-
370 isopropylmalate dehydratase involved in leucine biosynthesis, and PheA (Sll1662), prephenate dehydratase
371 involved in phenylalanine biosynthesis, remained unchanged in high copper-acclimated cells, unlike their mRNAs
372 that were up-regulated after the copper shock treatment (Giner-Lamia *et al.* 2014). Importantly, in acclimated
373 *Synechocystis* cells, SufA (FutA1, IdiA, Slr1295), SufB (Slr0074), SufC (Slr0477), SufD (Slr0076), and SufE
374 (Slr1419) were at the same levels as in the standard BG-11 medium. In contrast, corresponding mRNAs were up-
375 regulated in the shock-treated cells, both in *Synechocystis* (Giner-Lamia *et al.* 2014) and in *Synechococcus* (Stuart
376 *et al.* 2009). The results suggest the absence of the acute necessity for repair of the Fe-S clusters in acclimated
377 cells since the proteins involved in Fe-S cluster biogenesis (the *suf* system) were not differentially regulated.
378 Further, in copper shock-treated cells, in addition to damaging the Fe-S clusters, high $Cu^{2+}$ concentrations caused
379 the redox stress due to generation of ROS (Macomber *et al.* 2006; Macomber and Imlay 2009; Giner-Lamia *et al.*
380 2014; Huertas *et al.* 2014). The up-regulation of genes involved in ROS detoxification system as well as those
381 related to misfolded protein stress response was detected in shock-treated *Synechocystis* (Giner-Lamia *et al.* 2014)

382 and in *Synechococcus* (Stuart *et al.* 2009) cells. In contrast, in our study, chaperones (GroEL1, Slr2075 and GroES
383 Slr2075) and enzymes protecting proteins from the oxidative stress, like peroxiredoxins PrxII (Sll1621), 2-Cys-
384 prx (Sll0755), and NADP-thioredoxin reductase (Slr0600), remained at similar levels in H and S. Next, in the
385 shock-treated *Synechocystis* cells, the microarray investigation demonstrated downregulation of both carbon and
386 nitrogen metabolism (Giner-Lamia *et al.* 2014). In our experiment, the bicarbonate transport system BCT-1
387 (CmpB-D) diminished by 50% upon acclimation to high $Cu^{2+}$, but $CO_2$-uptake systems, NDH-$1_{3/4}$, $HCO_3^-$
388 transporter BicA, and GlgP (Sll1356) and GlgX (Slr1857) involved in glycogen metabolism were not affected.
389 Considering the nitrogen assimilation systems, in the shock-treated cells, genes encoding for glutamine synthetase
390 (*glnA*), the signal transduction protein PII (*glnB*) and high activity uptake ammonium permease (*amt1*) were down
391 regulated (Giner-Lamia *et al.* 2014). In contrast, in acclimated cells, GlnA, GlnB and Amt1 did not change, as
392 well as NtcA, the transcription factor regulating their expression (Osanai *et al.* 2007). Moreover, several other
393 proteins involved in uptake and assimilation of nitrogen, like glutamate-ammonia ligase (GlnN), subunits of
394 nitrate/nitrite transporter (NrtB, NrtC, NrtD), urea transporter UrtA, UrtC, UrtD) and urease (UreA), were
395 increased in H compared to S, while glutamine synthetase inactivation factors IF7 (GifA) and IF17 (GifB) were
396 distinctly decreased. The results suggest that nitrogen metabolism was activated in high copper-acclimated
397 *Synechocystis* cells. Porins also demonstrated dissimilar responses to high copper, depending on treatment. High
398 copper-dependent down-regulation of porins expression has been observed in various bacteria including *E. coli*
399 (Lutkenhaus *et al.* 1977), *Pseudomonas* (Teitzel *et al.* 2006), *Synechocystis* (Giner-Lamia *et al.* 2014) and marine
400 *Synechococcus* (Stuart *et al.* 2009). In our experiment, porins (Slr1908, Slr1841 and Slr1704) were up-regulated.
401 One of them, the hypothetical S-layer protein Slr1704, was among the most induced proteins in H compared to S.
402 By transcriptional profiling, Teitzeil *et al.* (2006) compared *Pseudomonas aeruginosa* cells subjected to
403 shock copper stress and after acclimation to higher copper concentrations. In addition to common features, the
404 important differences were observed between the two types of $Cu^{2+}$ stress. For example, the shock treatment induce
405 an oxidative stress response; which was not observed in the acclimated cells. Next, the *PA2505* gene encoding one
406 of the uncharacterized porins was strongly induced by long-term $Cu^{2+}$ exposure, similarly to up-regulation of
407 Slr1704 in acclimated *Synechocystis* cells. The proteome changes, described here, corroborated the notion that the

408 acclimation process had a profound impact on the response of *Synechocystis* to the high copper concentration, and
409 the slow exposure to increasing copper concentrations considerably alleviated the toxic effect of 5 μmol $l^{-1}$ $Cu^{2+}$.4

410 **Proteome adjustment to the $Cu^{2+}$ removal after the copper stress**

411 Comparison of protein amounts in cells after copper depletion in relation to those at high $Cu^{2+}$, D/H (Table
412 2), demonstrated *Synechocystis* proteome rearrangements in response to the removal of copper ions from the
413 medium. They are summarized in the Fig S3. As expected, cyt $c_{553}$ was strongly up-regulated corroborating the
414 activation of the *petJ* promoter, and the amounts of PC clearly decreased. However, PC remained at the slightly
415 elevated level compared to the standard conditions (D/S). CopR, CopS, CopM, CopA and CopB were also down-
416 regulated when the high copper stress was relieved (D/H) but, similarly to PC, not all of them returned to the
417 standard levels (D/S). Their remaining up-regulation indicated that 2 days in the $Cu^{2+}$-free medium was not enough
418 to deplete copper inside the cells. Many other proteins, like the bicarbonate transport system BCT-1 and most of
419 the enzymes related to nitrogen uptake and assimilation, which were mentioned above, restored their expression
420 to normal levels, or at least changed it toward the opposite direction after change of the media.

421 Noteworthy, our results demonstrated that some very important cellular systems became impaired by
422 gradual acclimation to high-copper conditions (see Table 1 and Fig.2). Revealing these systems was the main aim
423 of our investigation, since their suboptimal performance may have important consequences in biotechnological
424 applications. Several proteins of the photosynthesis machinery (ApcB, Slr1986; ApcC, Ssr3383; PsbE, Ssr3451;
425 PsaE, Ssr2831; PsaL, Slr1655 ) showed consistent negative changes during the whole experiment and were down-
426 regulated at the time point when the synthesis of the product should be on-going in the real biotechnological
427 experiment. Next, the cooperative down-regulation of the ribosomal proteins and regulators involved in translation
428 (IF-1, IF-2, IF-3 and the elongation factor P) indicated that the efficiency of protein synthesis was decreased which
429 might compromise the yield of the product of interest. The copper treatment caused also significant alterations in
430 the protein content of the cell surface layer, outer and plasma membranes. For example, porins Slr1908 and Slr1841
431 that were up-regulated in H, did not respond to the copper removal, and Slr1704 even further increased at this step.
432 The latter changes might create problems in the protein secretion if it is desired for the production process. Further,
433 the down-regulation of acyl-lipid desaturase DesC (Sll0541) could be a factor to consider the *petJ* promoter with

434 a caution in biotechnological production of fatty acids and lipids. A large group of proteins annotated as "unknown"
435 and "hypothetical" also responded strongly to the changes of copper concentration in the growth media (Table S2)
436 suggesting that so far unknown processes might be affected under the applied conditions.

437 The results presented in this paper contribute to the understanding of intracellular changes that occur in
438 *Synechocystis* during growth conditions applied to control the *petJ* promoter, and thus facilitate the successful
439 engineering of cyanobacterial cells for biotechnological purposes. Since the acclimation process significantly
440 alleviated the toxicity of the high copper concentration, $P_{PetJ}$. remains to be a useful inducible promoter if revealed
441 proteome alterations are irrelevant for the final goal. It would be interesting to know how the *Synechocystis*
442 proteome would respond to simulated use of the *petE* promoter which is repressed by the absence of the copper
443 ions and activated by their presence. Comparison of two systems might reveal novel mechanisms involved in
444 response of *Synechocystis* cells to excess and deprivation of copper in growth media.

445 **ACKNOWLEDGEMENTS**

446 The research leading to these results has received funding from the People Programme (Marie Curie Actions) of
447 the European Union's Seventh Framework Programme FP7/2007-2013/under REA Grants Agreement no. 317184
448 (M.A.). This material reflects only the authors' views and the European Union is not liable for any use that may
449 be made of the information therein. The authors also gratefully acknowledge the financial support from the
450 Academy of Finland Centre of Excellence Project number 307335, the Academy of Finland Project number
451 303757 (E.M.A.) and the Turku University Foundation project number 9925 (N.B.). Mass spectrometry analysis
452 was performed at the Turku Proteomics Facility, University of Turku and Åbo Akademi University, supported by
453 Biocenter Finland.

454 **CONFLICT OF INTEREST**

455 The authors declare no conflict of interest

456 **REFERENCES**

457 • Aro, E.M. 2016. From first generation biofuels to advanced solar biofuels. *Ambio* **45**: 24-31.

458 • Badarau, A. and Dennison, C. 2011. Thermodynamics of $Cu^{2+}$ and zinc distribution in the cyanobacterium
459 *Synechocystis* PCC 6803. *Proc Natl Acad Sci* **108**: 13007-13012.
460 • Bantscheff, M., Schirle, M., Sweetman, G., Rick, J. and Kuster, B. 2007. Quantitative mass spectrometry in
461 proteomics: a critical review. *Anal Bioanal Chem* **389**:1017-1031.
462 • Berla, B.M., Saha, R., Immethun, C.M., Maranas, C.D., Moon, T.S. and Pakrasi, H. 2013. Synthetic biology of
463 cyanobacteria: unique challenges and opportunities. *Front Microbiol* **4**: 246.
464 • Bersanini, L., Battchikova, N., Jokel, M., Rehman, A., Vass, I., Allahverdiyeva, Y., and Aro, E.M. 2014.
465 Flavodiiron protein Flv2/Flv4-related photoprotective mechanism dissipates excitation pressure of PSII in
466 cooperation with phycobilisomes in cyanobacteria. *Plant Physiol* **164**: 805-818.
467 • Bryan, S.J., Burroughs, N.J., Evered, C., Sacharz, J., Nenninger, A., Mullineaux, C.W. and Spence, E.M. 2011.
468 Loss of the SPHF homologue Slr1768 leads to a catastrophic failure in the maintenance of thylakoid membranes
469 in *Synechocystis* sp. PCC 6803. *PLoS One* **6**: e19625.
470 • Calderon, R.H., García-Cerdán, J.G., Malnoë, A., Cook, R., Russell, J.J., Gaw, C., Dent, R.M., de Vitry, C. and
471 Niyogi, K.K. 2013. A conserved rubredoxin is necessary for photosystem II accumulation in diverse oxygenic
472 photoautotrophs. *J Biol Chem* **288**: 26688-26696.
473 • De la Cerda, B., Castielli, O., Durán, R. V., Navarro, J. A., Hervás, M., and De la Rosa, M. A. 2007. A
474 proteomic approach to iron and copper homeostasis in cyanobacteria. *Brief Function Genom Proteom* **6:** 322-
475 329.
476 • Diaz, A., Navarro, F., Hervás, M., Navarro, J.A., Chávez, S., Florencio, F.J. and Miguel, A. 1994. Cloning and
477 correct expression in *E. coli* of the *petJ* gene encoding cytochrome $c_6$ from *Synechocystis* 6803. *FEBS Lett* **347**:
478 173-177.
479 • Dienst, D., Georg, J., Abts, T., Jakorew, L., Kuchmina, E., Börner, T., Wilde, A., Dühring, U., Enke, H. and
480 Hess, W.R. 2014. Transcriptomic response to prolonged ethanol production in the cyanobacterium
481 *Synechocystis* sp. PCC6803. *Biotechnol Biofuels* **7**: 21.

482 • Eisenhut, M., Georg, J., Klähn, S., Sakurai, I., Mustila, H., Zhang, P., Hess, W.R. and Aro, E.M. 2012. The
483 antisense RNA As1_flv4 in the cyanobacterium *Synechocystis* sp. PCC 6803 prevents premature expression of
484 the flv4-2 operon upon shift in inorganic carbon supply. *J Biol Chem* **287**: 33153-33162.
485 • Englund, E., Liang, F. and Lindberg, P. 2016. Evaluation of promoters and ribosome binding sites for
486 biotechnological applications in the unicellular cyanobacterium *Synechocystis* sp. PCC 6803. *Sci Rep* **6**:
487 e36640.
488 • Ferreira, E. A., Pacheco, C. C., Pinto, F., Pereira, J., Lamosa, P., Oliveira, P., Kirov, B., Jaramillo, A .and
489 Tamagnini, P. 2018. Expanding the toolbox for *Synechocystis* sp. PCC 6803: validation of replicative vectors
490 and characterization of a novel set of promoters. *Synth. Biol*. **3**: ysy014.
491 • Fulda, S., Huang, F., Nilsson, F., Hagemann, M. and Norling, B. 2000. Proteomics of *Synechocystis* sp. strain
492 PCC 6803. *FEBS J* **267**:5900-5907.
493 • Fulda, S., Norling, B., Schoor, A. and Hagemann, M. 2002. The Slr0924 protein of *Synechocystis* sp. strain
494 PCC 6803 resembles a subunit of the chloroplast protein import complex and is mainly localized in the
495 thylakoid lumen. *Plant Mol Biol* **49**: 107-118.
496 • Gandini, C., Schmidt, S.B., Husted, S., Schneider, A. and Leister, D. 2017. The transporter SynPAM71 is
497 located in the plasma membrane and thylakoids, and mediates manganese tolerance in *Synechocystis* PCC6803.
498 *New Phytol* **215**.
499 • Georg, J., Dienst, D., Schürgers, N., Wallne, T., Kopp, D., Stazic, D., Kuchmina, E., Klähn, S., Lokstein, H.,
500 Hess, W.R. and Wilde, A. 2014. The small regulatory RNA SyR1/PsrR1 controls photosynthetic functions in
501 cyanobacteria. *Plant Cell* **26**: 3661-3679.
502 • Giner-Lamia, J., López-Maury, L. and Florencio, F.J. 2014. Global transcriptional profiles of the $Cu^{2+}$
503 responses in the cyanobacterium *Synechocystis* sp. PCC 6803. *PloS One* **9**: e108912.
504 • Giner-Lamia, J., López-Maury, L. and Florencio, F.J. 2016. Ni interferes in the Cu-regulated transcriptional
505 switch *petJ*/*petE* in *Synechocystis* sp. PCC 6803. *FEBS Lett* **590**: 3639-3648.

506 • Giner-Lamia, J., López-Maury, L., Reyes, J.C. and Florencio, F.J. 2012. The CopRS two-component system is
507 responsible for resistance to $Cu^{2+}$ in the cyanobacterium *Synechocystis* sp. PCC 6803. *Plant Physiol* **159**: 1806-
508 1818.
509 • Giordano, M. and Wang, Q. 2018 Microalgae for Industrial Purposes. In: *Biomass and Green Chemistry* Ed
510 Vaz Jr. S. pp. 133-167. New York: Springer.
511 • Grouneva, I., Muth-Pawlak, D., Battchikova, N. and Aro, E.M. 2016. Changes in relative thylakoid protein
512 abundance induced by fluctuating light in the diatom *Thalassiosira pseudonana*. *J Proteome Res* **15**: 1649-
513 1658.
514 • Gudmundsson, S., Agudo, L. and Nogales, J. 2018. Applications of genome-scale metabolic models of
515 microalgae and cyanobacteria in biotechnology. In *Microalgae-Based Biofuels and Bioproducts* ed. Muñoz,
516 R., and Gonzalez-Fernandez, C. pp. 93-111 (Eds) Cambridge: Woodhead Publishing.
517 • Gudmundsson, S., and Nogales J. 2015. Cyanobacteria as photosynthetic biocatalysts: a systems biology
518 perspective. *Mol Biosyst* **11**: 60-70.
519 • Hagemann, M. and Hess, W.R.. 2018. Systems and synthetic biology for the biotechnological application of
520 cyanobacteria. *Curr Opin Biotech*.**49**: 94-99.
521 • Heidorn, T., Camsund, D., Huang, H.H., Lindberg, P., Oliveira, P., Stensjö, K. and Lindblad, P. 2010. Synthetic
522 biology in cyanobacteria engineering and analyzing novel functions. *Method Enzymol* **497**: 539-579.
523 • Huang, F., Hedman, E., Funk, C., Kieselbach, T., Schröder, W.P. and Norling, B. 2004. Isolation of outer
524 membrane of *Synechocystis* sp. PCC 6803 and its proteomic characterization. *Mol Cell Proteomics* **3**: 586-595.
525 • Huokko, T., Muth-Pawlak, D., Battchikova, N., Allahverdiyeva, Y. and Aro, E.M. 2017. Role of type 2 NAD
526 (P) H dehydrogenase NdbC in regulation of carbon allocation in *Synechocystis* 6803. *Plant Physiol,* 00398.
527 • Huertas, M., López-Maury, L., Giner-Lamia, J., Sánchez-Riego, A., and Florencio, F. 2014. Metals in
528 cyanobacteria: analysis of the copper, nickel, cobalt and arsenic homeostasis mechanisms. Life, **4**: 865-886.

529 • Jamers, A., Van der Ven. K., Moens, L., Robbens, J., Potters, G., Guisez, Y., Blust, R. and De Coen, W. 2006.
530 Effect of $Cu^{2+}$ exposure on gene expression profiles in *Chlamydomonas reinhardtii* based on microarray
531 analysis. *Aquat Toxicl* **80**: 249-260.
532 • Kaneko, T., Sato, S., Kotani, H., Tanaka, A., Asamizu, E., Nakamura,Y., Miyajima, N., Hirosawa, M., Sugiura,
533 M., Sasamoto, S. and Kimura, T. 1996. Sequence analysis of the genome of the unicellular cyanobacterium
534 Synechocystis sp. strain PCC6803. II. Sequence determination of the entire genome and assignment of potential
535 protein-coding regions. DNA Res **3**: 109-136.
536 • Khalil, A.S. and Collins, J.J. 2010. Synthetic biology: applications come of age. *Nat Rev Genet* **11**: 367.
537 • Klähn, S., Schaal, C., Georg, J., Baumgartner, D., Knippen, G., Hagemann, M., Muro-Pastor, A.M. and Hess,
538 W.R. 2015. The sRNA NsiR4 is involved in nitrogen assimilation control in cyanobacteria by targeting
539 glutamine synthetase inactivating factor IF7. *P Nat A Sci* **112**: 6243-6252.
540 • Kubota, H., Sakurai, I., Katayama, K., Mizusawa, N., Ohashi, S., Kobayashi, M., Zhang, P., Aro, E.M. and
541 Wada, H. 2010. Purification and characterization of photosystem I complex from *Synechocystis* sp. PCC 6803
542 by expressing histidine-tagged subunits. *BBA-Bioenergetics* **1797**: 98-105.
543 • Kuchmina, E., Wallner, T., Kryazhov, S., Zinchenko, V.V. and Wilde, A. 2012. An expression system for
544 regulated protein production in *Synechocystis* sp. PCC 6803 and its application for construction of a conditional
545 knockout of the ferrochelatase enzyme. *J Biotechnol* **162**: 75-80.
546 • Kumar, K.S., Dahms, H.U., Won, E.J., Lee, J.S. and Shin, K.H. 2015. Microalgae–A promising tool for heavy
547 metal remediation. *Ecotox Environ Safe* **113**: 329-352.
548 • Lutkenhaus, J.F. 1977. Role of a major outer membrane protein in *Escherichia coli*. *J Bacteriol* **131**: 631–637.
549 • Macomber, L., Rensing, C., and Imlay, J. A. 2007. Intracellular copper does not catalyze the formation of
550 oxidative DNA damage in *Escherichia coli*. *J bacteriol* **189**: 1616-1626.
551 • Macomber, L., and Imlay, J. A. (2009). The iron-sulfur clusters of dehydratases are primary intracellular targets
552 of copper toxicity. *Proc Natl Acad Sci* **106**: 8344-8349.

553 • Mitschke, J., Georg, J., Scholz, I., Sharma, C.M., Dienst, D., Bantscheff, J., Voß, B., Steglich, C., Wilde, A.,
554 Vogel, J. and Hess, W.R. 2011. An experimentally anchored map of transcriptional start sites in the model
555 cyanobacterium *Synechocystis* sp. PCC6803. *Proc Natl Acad Sci* **108**: 2124-2129.
556 • Murthy, H.N., Lee, E.J. and Paek, K.Y. 2014. Production of secondary metabolites from cell and organ cultures:
557 strategies and approaches for biomass improvement and metabolite accumulation. *Plant Cell Tiss Org* **118**: 1-
558 16.
559 • Osanai, T., Azuma, M. and Tanaka, K. 2007. Sugar catabolism regulated by light-and nitrogen-status in the
560 cyanobacterium *Synechocystis* sp. PCC 6803. *Photochem Photobio Sci* **6**: 508-514.
561 • Pade, N., Mikkat, S. and Hagemann, M. 2017. Ethanol, glycogen and glucosylglycerol represent competing
562 carbon pools in ethanol-producing cells of *Synechocystis* sp. PCC 6803 under high-salt conditions.
563 *Microbiology* **163**: 300-307.
564 • Parmar, A., Singh, N.K., Pandey, A., Gnansounou, E. and Madamwar, D. 2011. Cyanobacteria and microalgae:
565 a positive prospect for biofuels. *Bioresource Technol* **102**: 10163-10172.
566 • Pereira, S., Micheletti, E., Zille, A., Santos, A., Moradas-Ferreira, P., Tamagnini, P. and De Philippis, R. 2011.
567 Using extracellular polymeric substances (EPS)-producing cyanobacteria for the bioremediation of heavy
568 metals: do cations compete for the EPS functional groups and also accumulate inside the cell? *Microbiology.*
569 **157**: 451-458.
570 • Perkins, D.N., Pappin, D.J., Creasy, D.M. and Cottrell, J.S. 1999. Probability-based protein identification by
571 searching sequence databases using mass spectrometry data. Electrophoresis **20**: 3551-3567.
572 • Phillips, I. and Silver, P. 2006. A new biobrick assembly strategy designed for facile protein engineering.
573 *DSpace.*
574 • Pojidaeva, E.S., Malterer, S., Baik, A.S. and Sokolenko, A.V.. 2013. Inactivation of sll0136 gene in
575 *Synechocystis* sp. PCC 6803 results in the disturbance in protein biogenesis of photosynthetic complexes. *Russ*
576 *J Plant Physl* **60**: 511-517.

577 • Rast, A., Rengstl, B., Heinz, S., Kling, L., and Nickelsen, J. 2016. The role of Slr0151, a tetratricopeptide repeat
578 protein from *Synechocystis* sp. PCC 6803, during Photosystem II assembly and repair. *Front Plant Sci* **7**: e605.
579 • Reumann, S., Davila-Aponte, J. and Keegstra, K. 1999. The evolutionary origin of the protein-translocating
580 channel of chloroplastic envelope membranes: identification of a cyanobacterial homolog. *Proc Natl Acad Sci*
581 *USA* **96**: 784-789.
582 • Reyes, J.C., Muro-Pastor, M.I., and Florencio, F.J. 1997. Transcription of glutamine synthetase genes (*glnA*
583 and *glnN*) from the cyanobacterium *Synechocystis* sp. strain PCC 6803 is differently regulated in response to
584 nitrogen availability. *J Bacteriol* **179**: 2678-2689.
585 • Rippka, R., Deruelles, J., Waterbury, J.B., Herdman, M. and Stanier, R.Y. 1979. Generic assignments, strain
586 histories and properties of pure cultures of cyanobacteria. *Microbiology* **111**: 1-61.
587 • Sandmann, G. 1986. Formation of plastocyanin and cytochrome c-553 in different species of blue-green algae.
588 *Arch Microbiol* **145**: 76-79.
589 • Schuurmans, R.M., Matthijs, J.C.P. and Hellingwerf, K.J.. 2017. Transition from exponential to linear
590 photoautotrophic growth changes the physiology of *Synechocystis* sp. PCC 6803. *Photosynth Res* **132**: 69-82.
591 • Shavyrina, O.B., Gapochka, L.D. and Azovskii, A.I. 2001. Development of tolerance for copper in
592 cyanobacteria repeatedly exposed to its toxic effect. *Russ Ac Sc Bio Bulletin* **28**: 183-187.
593 • Stanier, R.Y., Kunisawa, R., Mandel, M. and Cohen-Bazire, G. 1971. Purification and properties of unicellular
594 blue-green algae (order Chroococcales). *Bacteriol Rev* **35**: 171-205.
595 • Stuart, R.K., Bundy, R., Buck, K., Ghassemain, M., Barbeau, K. and Palenik, B. 2017. Copper toxicity response
596 influences mesotrophic *Synechococcus* community structure. *Environ Microbiol* **19**: 756-769.
597 • Stuart, R.K., Dupont, C.L., Johnson, D.A., Paulsen, I.T. and Palenik, B. 2009. Coastal strains of marine
598 *Synechococcus* species exhibit increased tolerance to $Cu^{2+}$ shock and a distinctive transcriptional response
599 relative to those of open-ocean strains. *App Environ Microb* **75**: 5047-5057.

600 • Teitzel, G. M., Geddie, A., Susan, K., Kirisits, M. J., Whiteley, M., and Parsek, M. R. 2006 Survival and growth
601 in the presence of elevated copper: transcriptional profiling of copper-stressed *Pseudomonas aeruginosa*. *J*
602 *Bacteriol* **188**: 7242-7256.
603 • Tottey, S., Patterson, C.J., Banci, L., Bertini, I., Felli, I.C., Pavelkova, A., Dainty, S.J., Pernil, R., Waldron,
604 K.J., Foster, A.W. and Robinson, N.J. 2012 Cyanobacterial metallochaperone inhibits deleterious side reactions
605 of copper. *P Nat A Sci* **109**: 95-100.
606 • Tottey, S., Waldron, K.J., Firbank, S.J., Reale, B., Bessant, C., Sato, K., Cheek, T.R., Gray J, Banfield MJ,
607 Dennison C and Robinson N.J. 2008. Protein-folding location can regulate manganese-binding versus copper-
608 or zinc-binding. *Nature* **455**: 1138-1142.
609 • Trautmann, D., Voß, B., Wilde, A., Al-Babili, S. and Hess, W.R. 2012. Microevolution in cyanobacteria: re-
610 sequencing a motile substrain of *Synechocystis* sp. PCC 6803. *DNA Res* **19**: 435-448.
611 • Wang, X., Xiong, X., Sa, N., Roje, S. and Chen, S. 2016. Metabolic engineering of enhanced glycerol-3-
612 phosphate synthesis to increase lipid production in *Synechocystis* sp. PCC 6803. *Appl Microbiol Biot* **100**: 6091-
613 6101.
614 • Wegener, K.M., Welsh, E.A., Thornton, L.E., Keren, N., Jacobs, J.M., Hixson, K.K., Monroe, M.E., Camp,
615 D.G., Smith, R.D. and Pakrasi, H.B. 2008. High sensitivity proteomics assisted discovery of a novel operon
616 involved in the assembly of photosystem II, a membrane protein complex. *J Bio Chem* **283**: 27829-27837.
617 • Yang, H., Liao, L., Bo, T., Zhao, L., Sun, X., Lu, X., Norling, B. and Huang, F. 2014. Slr0151 in *Synechocystis*
618 sp. PCC 6803 is required for efficient repair of photosystem II under high-light condition. *J Integr Plant Biol*
619 **56**: 1136-1150.
620 • Yoshihara, S., Geng, X., Okamoto, S., Yura, K., Murata, T., Go ,M., Ohmori, M. and Ikeuchi, M., 2001.
621 Mutational analysis of genes involved in pilus structure, motility and transformation competency in the
622 unicellular motile cyanobacterium *Synechocystis* sp. PCC6803. *Plant Cell Physiol* **42**: 63-73.

623 • Yoshimura, H., Kaneko, Y., Ehira, S., Yoshihara, S., Ikeuchi, M. and Ohmori, M. 2010. CccS and CccP are
624 involved in construction of cell surface components in the cyanobacterium *Synechocystis* sp. strain PCC 6803.
625 *Plant Cell Physiol* **5**: 1163-1172.
626 • Zhang, L., McSpadden, B., Pakrasi, H.B. and Whitmarsh, J. 1992. $Cu^{2+}$-mediated regulation of cytochrome $c_{553}$
627 and plastocyanin in the cyanobacterium *Synechocystis* 6803. *J Bio Chem* **267**: 19054-19059.
628 • Zinchenko, V.V., Piven, I.V., Melnik, V. and Shestakov, S.V. 1999. Vectors for the complementation analysis
629 of cyanobacterial mutants. Russ J Genet **3**: 228-232.
630

631 TABLES AND TABLE LEGENDS

632 **Table 1:** Numbers of proteins which showed differential expression (FC of ± 1.40) at distinct phases of the
633 experiment. H/S: acclimation to high 5 µmol l-1 $Cu^{2+}$ (H) from standard condition (S); D/H: depletion of copper
634 from the 5 µmol $l^{-1}$ $Cu^{2+}$ (H) to $Cu^{2+}$-free BG-11 (D); D/S: Difference between $Cu^{2+}$-free BG-11 (D) condition and
635 standard BG-11 (S). The proteins were quantified with Anova <0.05.

636

| | H/S | D/H | D/S |
|---|---|---|---|
| UP | 103 | 30 | 70 |
| DOWN | 62 | 77 | 75 |

637

638 **Table**2: The list of *Synechocystis* proteins which demonstrated altered protein expression under different copper
639 availability Values are shown in blue for FC > + 1.40 and in magenta for FC<-1.40. Values obtained with Anova
640 <0.05 are reported in bold. H/S: differential protein expression during acclimation of cells to high 5 µmol $l^{-1}$ $Cu^{2+}$
641 (H) from standard condition (S) which would repress the P*petJ* promoter. D/H: significant proteome changes due
642 to depletion of copper from the medium (D) ) which would activate the P*petJ* promoter. D/S: ultimate protein
643 changes, caused by extreme $Cu^{2+}$ concentrations which should be used to control the petJ promoter, were
644 determined by comparison of protein expression between $Cu^{2+}$-free BG-11 (D) condition and standard BG-11
645 (S).

| *ORF* | *gene* | H/S | D/H | D/S | Description |
|---|---|---|---|---|---|
| | | | | | Cu homeostasis |
| *slr6040; sll0789* | *copR* | **40.84** | **-13.83** | **2.95** | two-component response regulator OmpR subfamily |
| *slr6041; sll0790* | *copS* | **3.48** | **-2.75** | 1.26 | two-component sensor histidine kinase |
| *slr6039; sll0788* | *copM* | **25.20** | **-12.06** | **2.09** | hypothetical protein |
| *slr6042* | *copB* | **10.66** | **-7.53** | **1.42** | cation efflux system protein, part of RND system |
| *slr6044* | *copC* | **4.39** | **-2.17** | **2.03** | efflux RND system outer menbrane protein |
| *slr6043* | *copA* | **1.36** | **-2.60** | **-1.91** | probable cation efflux RND system protein |
| *ssr2857* | *atx1* | **1.52** | -1.12 | **1.36** | small soluble copper metallochaperone |
| | | | | | Light harvesting and photosynthesis |
| *sll0199* | *petE* | **1.89** | **-1.54** | **1.23** | plastocyanin |
| *sll1796* | *petJ* | **-2.43** | **3.54** | 1.46 | cytochrome $c_{553}$ |
| *slr1986* | *apcB* | **-1.32** | -1.06 | **-1.40** | allophycocyanin beta subunit |
| *ssr3383* | *apcC* | **-1.29** | -1.12 | **-1.45** | phycobilisome small core linker polypeptide |

| | | | | | |
|---|---|---|---|---|---|
| *sll1579* | *cpcC2* | **-1.37** | -1.06 | **-1.45** | phycobilisome rod linker polypeptide |
| *ssr3451* | *psbE* | -1.19 | -1.21 | **-1.43** | cytochrome b559 alpha subunit |
| *slr0342* | *petB* | **-1.44** | 1.03 | **-1.41** | cytochrome $b_6$ |
| *ssr2831* | *psaE* | **-1.45** | -1.11 | **-1.61** | photosystem I subunit IV |
| *slr1655* | *psaL* | **-1.44** | -1.03 | **-1.48** | photosystem I subunit XI |
| *sll1325* | *atpD* | -1.52 | 1.09 | **-1.39** | ATP synthase delta chain of CF(1) |
| *ssl0020* | *fed1* | **1.70** | -1.31 | 1.30 | ferredoxin I |
| | | | Chlorophyll biosynthesis | | |
| *sll1185* | *hemF* | **-1.40** | 1.01 | **-1.39** | coproporphyrinogen III oxidase |
| *sll0017* | *hemL* | **-1.65** | **1.15** | **-1.43** | glutamate-1-semialdehyde aminomutase |
| *sll1994* | *hemB* | **-1.41** | **1.39** | -1.01 | porphobilinogen synthase |
| *sll1091* | *chlP* | **-1.49** | 1.08 | **-1.39** | geranylgeranyl hydrogenase |
| *sll1184* | *hox1* | **-1.56** | **1.31** | -1.19 | heme oxygenase |
| *slr0116* | *pcyA* | -1.08 | **-1.30** | **-1.41** | phycocyanobilin:ferredoxin oxidoreductase |
| | | | Photoprotection and regulation of photosynthesis | | |
| *slr0144* | | **1.65** | -1.10 | **1.51** | component of the PSII assembly proteins operon |
| *slr0147* | | **1.59** | -1.13 | **1.40** | component of the PSII assembly proteins operon |
| *slr0149* | | **1.42** | **-1.22** | **1.16** | component of the PSII assembly proteins operon |
| *slr0151* | | **1.42** | **-1.25** | 1.13 | component of the PSII assembly proteins operon |
| *sll0219* | *flv2* | **-1.80** | **1.83** | 1.02 | flavodiiron protein 2 |
| *sll0217* | *flv4* | **-1.73** | **1.49** | -1.16 | flavodiiron protein 4 |
| *sll1224* | *hoxY* | **1.35** | **-1.69** | -1.25 | bidirectional hydrogenase hydrogenase subunit |
| *slr1768* | | **1.66** | **-1.28** | **1.30** | unknown protein |
| *slr1743* | *ndbB* | **1.48** | **-1.37** | 1.08 | type-2 NADH dehydrogenase |
| *sll0223* | *ndhB* | 1.11 | **-1.40** | **-1.27** | NDH-1 subunit B |
| *sll1262* | *ndhN* | **1.52** | **-1.59** | -1.04 | NDH-1 subunit N |
| *ssl1690* | *ndhO* | **1.56** | **-1.22** | **1.28** | NDH-1 subunit O |
| *slr2033* | *rubA* | **1.51** | **-1.19** | **1.27** | rubredoxin A |
| | | | Carbon metabolism | | |
| *slr0041* | *cmpB* | **-1.99** | **2.20** | 1.11 | $CO_2$ transport system permease protein |
| *slr0043* | *cmpC* | **-2.56** | **2.27** | -1.13 | $CO_2$ transport system ATP-binding protein |
| *slr0044* | *cmpD* | **-1.60** | **1.29** | **-1.24** | bicarbonate transport system ATP-binding protein |
| *sll0934* | *ccmA* | **-1.33** | -1.07 | **-1.42** | carboxysome formation protein A |
| *slr1839* | *ccmK4* | **-1.53** | 1.20 | **-1.28** | $CO_2$ concentrating mechanism protein K4 |
| *sll1028* | *ccmK2* | **1.51** | **1.50** | **2.27** | $CO_2$ concentrating mechanism protein K2 |

| | | | | | |
|---|---|---|---|---|---|
| *sll1031* | *ccmM* | **-1.24** | **-1.16** | **-1.44** | $CO_2$ concentrating mechanism protein M |
| *sll0891* | *citH* | **1.42** | 1.04 | **1.47** | malate dehydrogenase |
| *sll1557* | *sucD* | **1.39** | **-1.52** | -1.09 | succinyl-CoA synthetase alpha chain |
| *slr0952* | *fbp* | -1.08 | **-1.32** | **-1.42** | fructose-1,6-bisphosphatase |
| *sll0395* | *pmg* | **1.24** | **-1.44** | **-1.17** | phosphoglycerate mutase |
| *sll0807* | *cfxE* | **1.44** | 1.11 | **1.60** | pentose-5-phosphate-3-epimerase |
| *slr1448* | *cscK* | **1.31** | **-1.47** | -1.12 | fructokinase |
| *slr0301* | *ppsA* | **1.55** | -1.06 | **1.46** | phosphoenolpyruvate synthase |
| *sll1358* | *mncA* | **1.52** | **-1.14** | **1.34** | putative oxalate decarboxylas |
| | | | | Nitrogen metabolism | |
| *slr0288* | *glnN* | **3.72** | -1.38 | **2.69** | glutamate--ammonia ligase |
| *sll1515* | *gifB* | **-1.67** | -1.06 | **-1.77** | glutamine synthetase inactivating factor IF17 |
| *ssl1911* | *gifA* | **-16.03** | **2.33** | **-6.88** | glutamine synthetase inactivating factor IF7 |
| *sll1450* | *nrtA* | **1.11** | **-1.52** | **-1.37** | nitrate/nitrite transporter substrate-binding protein |
| *sll1451* | *nrtB* | **2.12** | **-2.22** | -1.05 | nitrate/nitrite transporter permease protein |
| *sll1452* | *nrtC* | **2.57** | **-2.11** | 1.22 | nitrate/nitrite transporter ATP-binding protein |
| *sll1453* | *nrtD* | **3.31** | **-3.05** | 1.08 | nitrate/nitrite transport system ATP-binding protein |
| *slr0898* | *nirA* | **1.62** | **-1.57** | 1.03 | ferredoxin-nitrite reductase |
| *slr0447* | *urtA* | **2.03** | -1.12 | 1.82 | urea transport system substrate-binding protein |
| *slr1201* | *urtC* | **1.49** | **-1.34** | 1.12 | urea transport system permease protein |
| *sll0764* | *urtD* | **1.52** | **-1.66** | -1.10 | urea transport system ATP-binding protein |
| *slr1256* | *ureA* | **2.51** | 1.35 | **3.40** | urease gamma subunit |
| *sll1750* | *ureC* | **1.33** | **-1.50** | **-1.13** | urease alpha subunit |
| *sll0643* | *ureG* | **-1.55** | 1.23 | **-1.25** | urease accessory protein G |
| *slr0899* | *cynS* | **1.63** | **-1.94** | -1.19 | cyanate lyase |
| *sll0450* | *norB* | **1.46** | **-1.35** | 1.08 | cytochrome b subunit of nitric oxide reductase |
| *sll0100* | *ama* | 1.32 | 1.32 | **1.75** | N-acyl-L-amino acid amidohydrolase |
| *slr1653* | | **1.41** | **-1.66** | -1.18 | N-acyl-L-amino acid amidohydrolase |
| | | | | Protein synthesis | |
| *sll1244* | *rpl9* | **-1.53** | 1.15 | **-1.33** | 50S ribosomal protein L9 |
| *sll1819* | *rpl17* | **-1.28** | **-1.23** | **-1.58** | 50S ribosomal protein L17 |
| *ssr2799* | *rpl27* | **-1.54** | **-1.33** | **-2.04** | 50S ribosomal protein L27 |
| *ssr1604* | *rpl28* | **-1.32** | **-1.29** | **-1.70** | 50S ribosomal protein L28 |
| *ssl3445* | *rpl31* | **-1.20** | **-1.20** | **-1.44** | 50S ribosomal protein L31 |
| *ssl1426* | *rpl35* | -1.05 | **-1.63** | **-1.71** | 50S ribosomal protein L35 |

| | | | | | |
|---|---|---|---|---|---|
| *slr0469* | *rps4* | **-1.42** | -1.17 | **-1.66** | 30S ribosomal protein S4 |
| *sll1822* | *rps9* | **-1.18** | **-1.21** | **-1.43** | 30S ribosomal protein S9 |
| *sll1817* | *rps11* | -1.04 | **-1.47** | **-1.53** | 30S ribosomal protein S11 |
| *sll1816* | *rps13* | **-1.45** | -1.12 | **-1.63** | 30S ribosomal protein S13 |
| *ssl3437* | *rps17* | **-1.17** | **-1.47** | **-1.73** | 30S ribosomal protein S17 |
| *ssl3432* | *rps19* | -1.23 | **-1.87** | **-2.30** | 30S ribosomal protein S19 |
| *ssl3441* | *infA* | -1.01 | **-1.54** | **-1.56** | initiation factor IF-1 |
| *slr0744* | *infB* | -1.10 | **-1.29** | **-1.43** | initiation factor IF-2 |
| *slr0974* | *infC* | 1.06 | **-1.62** | **-1.54** | initiation factor IF-3 |
| *slr0434* | *efp* | **-1.56** | 1.07 | **-1.46** | elongation factor P |
| *sll0136* | *pepP* | **-1.38** | -1.09 | **-1.50** | aminopeptidase P |
| *slr1331* | *ymxG* | 1.42 | 1.11 | **1.58** | periplasmic processing protease |
| *slr1228* | *prfC* | **1.41** | **-1.31** | 1.08 | peptide-chain-release factor 3 |
| *slr0958* | *cysS* | **-1.51** | 1.73 | 1.15 | cysteinyl-tRNA synthetase |
| | | | | | Cellular periphery |
| *slr1704* | | **36.15** | 1.49 | **53.90** | hypothetical S-layer protein |
| *slr1908* | | **1.79** | -1.06 | **1.69** | probable porin |
| *slr1841* | | 1.76 | 1.06 | **1.86** | probable porin |
| *slr1277* | *pilQ* | **1.62** | 1.74 | **2.82** | pilus assembly protein homologous to general secretion pathway protein D |
| *slr1227* | SynToc75 | **1.50** | 1.07 | **1.41** | outer envelope membrane protein |
| *slr1668* | *cccP* | **1.94** | **-2.03** | -1.05 | periplasmic protein involved in cell surface components and biofilm syntesis |
| *slr0017* | *murA* | **-1.87** | **1.41** | **-1.33** | UDP-N-acetylglucosamine 1-carboxyvinyltransferase |
| *slr1656* | *murG* | 3.25 | 3.00 | **9.76** | UDP-N-acetylglucosamine--N-acetylmuramyl-(pentapeptide) pyrophosphoryl -undecaprenol N-acetylglucosamine transferase |
| *sll0899* | *glmU* | **-1.60** | 1.12 | **-1.44** | UDP-N-acetylglucosamine pyrophosphorylase |
| *slr0776* | *lpxD* | 1.16 | **1.26** | **1.46** | UDP-3-o-[3-hydroxymyristoyl] glucosamine n-acyltransferase |
| *sll0575* | *rfbB* | **-1.47** | 1.26 | -1.17 | probable lipopolysaccharide ABC transporter ATP binding subunit |
| *sll0640* | *sac1* | -1.14 | **-1.23** | **-1.40** | probable sodium/sulfate symporter |
| *slr1881* | *natE* | -1.01 | **-1.43** | **-1.45** | ATP-binding subunit of the ABC-type Nat permease for neutral amino acids |
| *slr0798* | *ziaA* | **-3.45** | -1.17 | **-4.05** | zinc-transporting P-type ATPase (zinc efflux pump) involved in zinc tolerance |
| *slr1615* | *rfbE* | **1.91** | -1.15 | 1.66 | perosamine synthetase |

| | | | | | |
|---|---|---|---|---|---|
| *slr2015* | *pilA9* | **-1.23** | **1.44** | 1.17 | type 4 pilin-like protein, essential for motility |
| | | | | | Other |
| *sll0094* | *hik37* | **1.66** | **-1.29** | 1.28 | two-component sensor histidine kinase |
| *sll1473* | *hik32* | -1.05 | **1.60** | **1.53** | phytochrome-like sensor histidine kinase |
| *slr1982* | *rre21* | -1.39 | **1.77** | 1.28 | two-component response regulator CheY family |
| *slr1859* | | **1.33** | **1.50** | **1.99** | anti-sigma f factor antagonist |
| *slr2075* | *groES* | **-1.55** | 1.15 | **-1.35** | 10kD chaperonin- GroES |
| *slr0093* | *dnaJ2* | 1.16 | **-1.47** | **-1.28** | DnaJ, heat shock protein 40, molecular chaperone |
| *slr1562* | *grxB* | **1.66** | 1.04 | **1.72** | glutaredoxin |
| *sll1545* | *gst1* | **1.21** | **-1.43** | **-1.18** | glutathione S-transferase |
| *ssr0330* | *ftrV* | -1.12 | **-1.25** | **-1.41** | FTR-ferredoxin-thioredoxin reductase, variab chain |
| *sll1341* | *bfrA* | **1.25** | **-1.48** | **-1.19** | bacterioferritin |
| *ssl2667* | *nifU* | -1.13 | **2.17** | **1.91** | iron-sulfur clusters assembly factor |
| *slr2131* | *acrF* | **-1.37** | -1.03 | **-1.41** | RND multidrug efflux transporter |
| *sll1814* | *secY* | **-1.40** | -1.00 | **-1.40** | preprotein translocase SecY subunit |
| *sll1181* | *hlyD* | **-1.42** | 1.09 | **-1.30** | similar to hemolysin secretion protein |
| *slr1779* | *pdxJ* | -1.03 | **-1.35** | **-1.40** | pyridoxal phosphate biosynthetic protein PdxJ |
| *slr0633* | *thiG* | **-1.42** | 1.20 | -1.18 | thiamine biosynthesis protein ThiG |
| *sll0541* | *desC* | **-1.98** | **-1.41** | **-2.79** | acyl-lipid desaturase (delta 9) |

646

647 **FIGURE LEGENDS**

648 **Figure 1**: Schematic representation of $Cu^{2+}$ changes in growth media during the experiment. The details are
649 described in the Materials and Methods. Samples analysed by quantitative label-free LC-MS/MS represent
650 proteomes of cells grown in standard BG-11 (S), at high $Cu^{2+}$ (H) and in $Cu^{2+}$ -depleted (D) conditions.

651 **Figure 2**: Schematic representation of background changes occurring in *Synechocystis* proteome under a
652 subjective biotechnological applications using the *petJ* promoter. Cells were first acclimated to 5 µmol $l^{-1}$ $Cu^{2+}$
653 and then shifted to $Cu^{2+}$ free medium. Protein which were differentially regulated at the end of the experiment
654 (D) compared to the standard condition (S) are shown in blue (up-regulated) and magenta (down-regulated). The
655 FC threshold value is ± 1.40

656

657 **SUPPLEMENTARY FILE:**

658 **Table S1**

659 **1**_Combined table of differential protein expression: Table of differential protein expression where results
660 presented in sheets 2, 3 and 4 are combined. H/S: differential protein expression resulting from acclimation of
661 cells to high 5 µmol $l^{-1}$ $Cu^{2+}$ (H) from standard condition (S); D/H: significant proteome changes due to
662 subsequent depletion of copper from the medium (D); D/S: final proteome changes caused by treatment of cells
663 with extreme $Cu^{2+}$ concentrations. Only proteins with Anova <0.05 in at least one phase are reported;
664 Anova<0.05 are in blue and Anova and FC of respective proteins are in bold. The threshold for significantly
665 altered expression (FC) was ± 1.40. Differential expression values over +1.40 are in blue, the ones below -1.40
666 are in magenta. For each quantified protein, the number of peptides, Anova and FC are reported.

667 **2**_H/S: Quantitation of changes in protein amounts during acclimation of cells to high 5 µmol $l^{-1}$ $Cu^{2+}$ (H) from
668 standard condition (S). FC is marked in blue if FC>1.40 or in magenta if FC< -1.40. For each quantified protein,
669 the number of peptides, Anova and FC reported. Anova<0.05 are in blue.

670 **3**_D/H: Quantitation of changes in protein amounts after shift of cells from BG-11 supplemented with 5 µmol $l^{-1}$
671 $Cu^{2+}$ (H) to $Cu^{2+}$ - free BG-11 (D). FC is marked in blue if FC>1.40 or in magenta if FC< -1.40. For each
672 quantified protein, the number of peptides, Anova and FC reported. Anova<0.05 are in blue.

673 **4**_D/S: Calculation of changes in protein amounts in cells subjected to $Cu^{2+}$ treatment (gradual adaptation to 5
674 µmol $l^{-1}Cu^{2+}$ followed by shift to $Cu^{2+}$ depleted condition). FC is marked in blue if FC>1.40 or in magenta if
675 FC< -1.40. For each quantified protein, the number of peptides, Anova and FC reported. Anova<0.05 are in blue.

676 **Table S2**

677 The list of *Synechocystis* hypothetical and unknown proteins which demonstrated altered protein expression
678 upon repression and activation of the *petJ* promoter. Values are shown in blue for FC > + 1.40 and in magenta
679 for FC<-1.40. Values obtained with Anova <0.05 are reported in bold. H/S: differential protein expression
680 during acclimation of cells to high 5 µmol $l^{-1}$ $Cu^{2+}$ (H) from standard condition (S); D/H: significant proteome

681 changes due to depletion of copper from the medium (D); D/S: ultimate protein changes, caused by treatment of
682 cells with 5 µmol $l^{-1}$ $Cu^{2+}$ followed by copper depletion, were determined by comparison of protein expression
683 between $Cu^{2+}$-free BG-11 (D) condition and standard BG-11 (S).

684 **Figure S1**

685 Growth curves of *Synechocystis* cells in standard BG-11 (green line) or subjected to the $Cu^{2+}$ treatment.
686 Acclimation of cells to the high $Cu^{2+}$ concentration (black line) was started in BG-11 medium containing 1 µmol
687 $l^{-1}$ $Cu^{2+}$ and followed by step-wise addition of 2.5 µmol $l^{-1}$ and 5 µmol $l^{-1}$ $Cu^{2+}$ $CuSO_4$ (marked by arrows). At the
688 2nd step of the experiment, the cells acclimated to high $Cu^{2+}$ were washed with $Cu^{2+}$ - free BG-11 medium
689 (dotted vertical line) and grown further in this medium for two days (blue line).

690 **Figure S2**

691 Schematic representation of changes occurring in *Synechocystis* during acclimation to increasing copper
692 concentration (H/S) which is based on data reported in Table 1, 3rd column. Up-regulated proteins, with FC > +
693 1.40, are shown in turquoise. Down-regulated proteins, with FC<-1.40 are shown in magenta. Only proteins with
694 Anova <0.05 are reported in colour.

695 **Figure S3**

696 Schematic representation of changes occurring in *Synechocystis* when high copper-acclimated cells were shifted
697 to $Cu^{2+}$-free BG-11 (D/H) which is based on data reported in Table 1, 4rd column. Up-regulated proteins, with
698 FC > + 1.40, are shown in turquoise. Down-regulated proteins, with FC<-1.40 are shown in magenta. Only
699 proteins with Anova <0.05 are reported in colour.

700

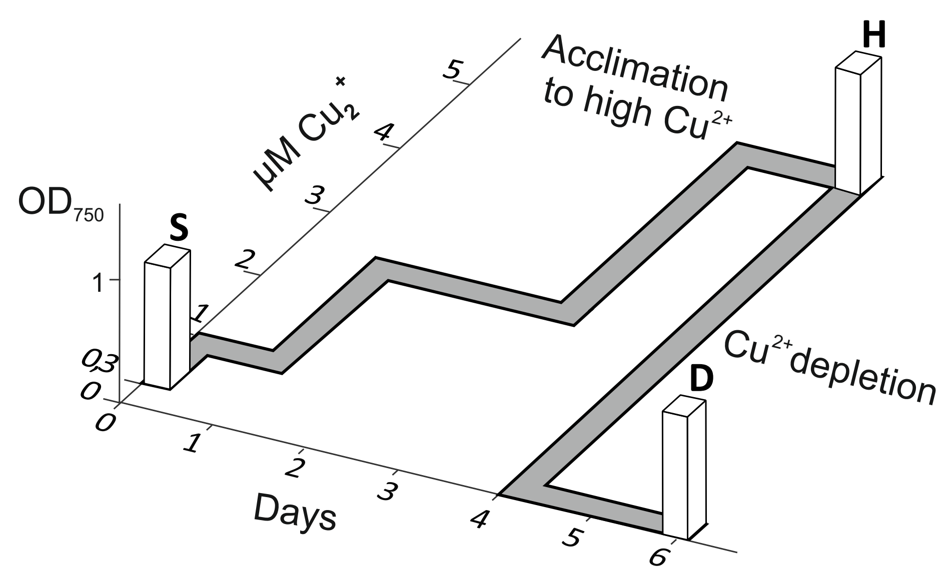

OD750
S
1
0.3
0
μM Cu2+
1
2
3
4
5
Acclimation
to high Cu2+
H
Cu2+ depletion
D
0
1
2
3
4
5
6
Days

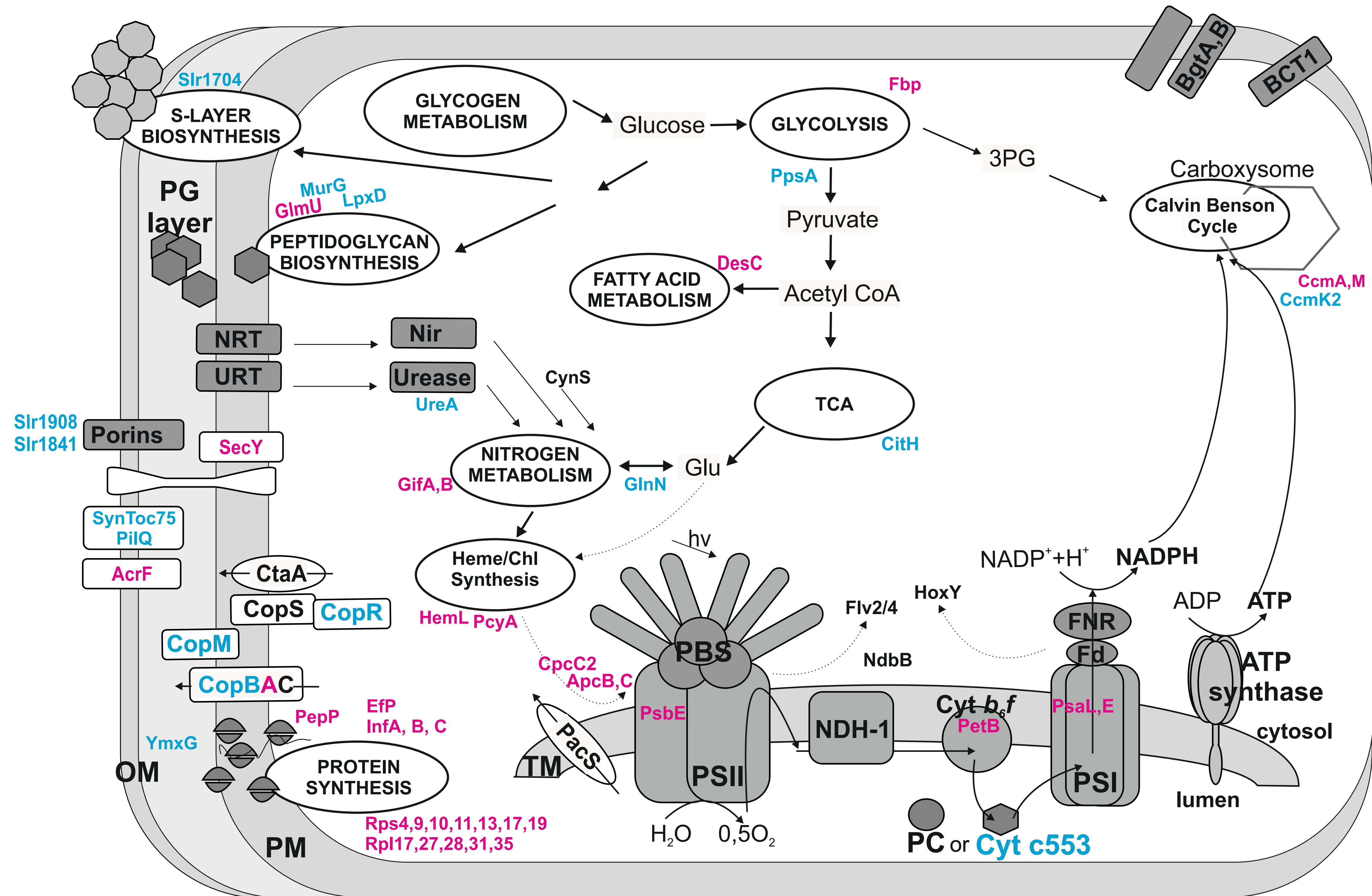

Slr1704
S-LAYER BIOSYNTHESIS
GLYCOGEN METABOLISM
Glucose
GLYCOLYSIS
Fbp
BgtA,B
BCT1
3PG
Carboxysome
Calvin Benson Cycle
PpsA
Pyruvate
PG layer
MurG
GlmU
LpxD
PEPTIDOGLYCAN BIOSYNTHESIS
DesC
FATTY ACID METABOLISM
Acetyl CoA
CcmA,M
CcmK2
NRT
Nir
URT
Urease
UreA
CynS
TCA
CitH
Slr1908
Slr1841
Porins
SecY
NITROGEN METABOLISM
GifA,B
Glu
GlnN
SynToc75
PilQ
AcrF
CtaA
Heme/Chl Synthesis
hv
NADP⁺+H⁺
NADPH
CopS
CopR
HemL
PcyA
Flv2/4
HoxY
ADP
ATP
CopM
PBS
NdbB
FNR
Fd
ATP synthase
CopBAC
CpcC2
ApcB,C
PsbE
Cyt b6f
PetB
PsaL,E
EfP
InfA, B, C
PepP
NDH-1
cytosol
YmxG
OM
TM
PacS
PSII
PSI
PROTEIN SYNTHESIS
lumen
Rps4,9,10,11,13,17,19
Rpl17,27,28,31,35
$H_2O$
$0,5O_2$
PC or Cyt c553
PM